Cell Capture

DOI: 10.1002/anie.201005853

Highly Efficient Capture of Circulating Tumor Cells by Using Nanostructured Silicon Substrates with Integrated Chaotic Micromixers**

Shutao Wang, Kan Liu, Jian Liu, Zeta T.-F. Yu, Xiaowen Xu, Libo Zhao, Tom Lee, Eun Kyung Lee, Jean Reiss, Yi-Kuen Lee, Leland W. K. Chung, Jiaoti Huang, Matthew Rettig, David Seligson, Kumaran N. Duraiswamy, Clifton K.-F. Shen,* and Hsian-Rong Tseng**

Metastases are the most common cause of cancer-related death in patients with solid tumors.[1–4] A considerable body of evidence indicates that tumor cells are shed from a primary tumor mass at the earliest stages of malignant progression.[5–7] These "break-away" circulating tumor cells (CTCs)[8–11] enter the blood stream and travel to different tissues of the body, as a critical route for cancer metastasis. The current gold standard for determining tumor status requires invasive biopsy and subsequent genetic and proteomic analysis of biopsy samples. Alternatively, CTC measurement and analysis can be regarded as a "liquid biopsy" of the tumor, providing insight into tumor biology in the critical window where intervention could actually make a difference. However, detection and characterization of CTCs has been technically challenging owing to their extremely low number in the bloodstream. CTCs are often found in the blood of patients with metastatic cancer, in only up to hundreds of cells mL^{-1}, whereas common blood cells exist in high numbers ($>10^9$ cells mL^{-1}). Over the past decade, a diverse suite of technologies[8,12–17] have been evolving to meet the challenge of counting and isolating CTCs from patient blood samples. Many employ different enrichment mechanisms, such as immunomagnetic separation based on capture-agent-labeled magnetic beads,[8,16] microfluidics-based technologies[12,14,17] that enhance cell-surface contacts, and microfilter devices[13] that isolate CTCs based on size difference. The sensitivity of these emerging technologies, which is critical to their clinical utility for detecting early cancer progression (e.g., tumor invasion of vascular systems), relies on the degree of enrichment of CTCs.

Recently, we discovered that a 3D-nanostructured substrate[18] coated with cancer-cell capture agents[19,20] (i.e., epithelial cell adhesion molecule antibody, anti-EpCAM) exhibits significantly improved cell-capture efficiency owing to its enhanced local topographic interactions[21] between the silicon nanopillar (SiNP) substrates and nanoscale cellular surface components (e.g., microvilli and filopodia). Such a high-affinity cell assay can be employed to recover cancer cells from spiked whole-blood samples, in a stationary device setting,[18] with cell-capture efficiency ranging from 40 to 70%. On the basis of this stationary cell-capture assay, we anticipated that further improvement of cell-capture performance can be achieved by increasing cell–substrate contact frequency. By integrating a simple but powerful fluidic handling system, namely a chaotic mixing channel,[22] with a patterned nanostructured substrate, highly efficient CTC capture can be realized by the synergistic effects of enhanced cell–substrate contact frequency as well as affinity. Although there are several microfluidic platforms[12,14,17] capable of achieving improved CTC-capture efficiency, the micropillar-based CTC-capture technologies[12,17] suffer from depth of field issues thus requiring multiple cross-sectional imaging scans to avoid out-of-focus or superimposed images of device-immobilized CTCs because of to the vertical depth of the

[*] Dr. S. T. Wang[+]
Beijing National Laboratory for Molecular Sciences
Key Laboratory of Organic Solids, Institute of Chemistry
Chinese Academy of Sciences, Beijing (P. R. China)
Dr. K. Liu[+]
College of Electronics and Information Engineering
Wuhan Textile University, Wuhan (P. R. China)
J. Reiss, Prof. J. Huang, Prof. D. Seligson
Department of Pathology and Laboratory Medicine
University of California, Los Angeles (USA)
Prof. M. Rettig
Department of Urology, University of California, Los Angeles (USA)
Prof. Y.-K. Lee
Department of Mechanical Engineering
The Hong Kong University of Science and Technology (Hong Kong)
Dr. J. Liu,[+] Prof. L. W. K. Chung
Uro-oncology Research Program, Samuel Oschin Comprehensive Cancer Institute, Cedars Sinai Medical Center
Los Angeles (USA)
Dr. S. T. Wang,[+] Dr. K. Liu,[+] Dr. J. Liu,[+] Dr. Z. T.-F. Yu, X. Xu, L. Zhao, T. Lee, Dr. E. K. Lee, Dr. K. N. Duraiswamy, Prof. C. K.-F. Shen, Prof. H.-R. Tseng
Department of Molecular and Medical Pharmacology, Crump Institute for Molecular Imaging (CIMI), California NanoSystems Institute (CNSI), Institute for Molecular Medicine (IMED)
University of California Los Angeles
570 Westwood Plaza, Building 114, Los Angeles, CA 90095-1770 (USA)
Fax: (+1) 310-206-8975
E-mail: kumar.duraiswamy@cytoscale.com
kshen@mednet.ucla.edu
hrtseng@mednet.ucla.edu
Homepage: http://labs.pharmacology.ucla.edu/tsenglab/
[+] These authors contributed equally to this work.

[**] This research was supported by the NIH IMAT Program (R21A151159-01) and a Prostate Cancer Foundation Creativity Award. We thank Prof. Allan Pantuck from the UCLA Urology Department for providing CTC blood samples.
Supporting information for this article is available on the WWW under http://dx.doi.org/10.1002/anie.201005853.

device features. The microfluidic device[14] with an integrated conductivity sensor provides the significant advantage of label-free CTC detection. However, whether the lack of cellular morphology influences pathologic characterization remains to be determined.

Herein we introduce a new CTC-capture platform that integrates two functional components (Figure 1): 1) a patterned SiNP substrate with anti-EpCAM coating for recognizing/capturing EpCAM-expressing cells, and 2) an overlaid polydimethylsiloxane (PDMS) chip with a serpentine chaotic mixing channel[22–27] that encourages increased cell–substrate contact frequency. When a blood sample containing CTCs flows through the device, the embedded chevron-shaped micropatterns on the channel roof induce vertical flow long were chemically etched onto a serpentine pattern defined by photolithography. According to the previously established method,[18] a streptavidin coating was introduced onto the patterned SiNP substrate using N-hydroxysuccinimide (NHS)/maleimide chemistry.[12,29] The PDMS chip with an 88 cm long chaotic mixing channel ($w\,h = 1000 \times 100$ μm) was produced by soft-lithography using a replicate on a silicon wafer. According to the theoretical model,[22] such a chaotic mixer can induce vertical flow of the blood, leading to significant enhancement in cell–substrate contact frequency compared to a static setting (see Supporting Information). A chip holder made of polyacrylate was designed and fabricated to sandwich the two functional components together. Prior to cell-capture experiments, 100 μL of biotinylated anti-EpCAM (10 μg mL^{-1}, R&D Systems) was introduced onto the integrated device for antibody coating. A digital pressure regulator was utilized to control the flow rates of 1) cell suspensions or blood samples, 2) fixation and permeabilization agents, and 3) immuno- and nuclear staining agents introduced sequentially into the integrated devices during the studies.

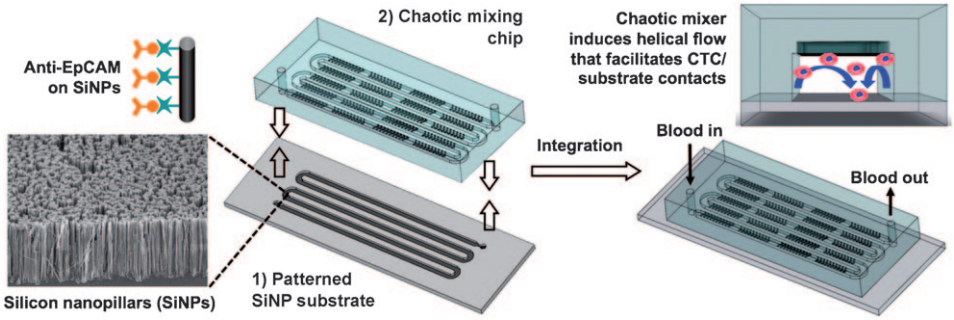

Figure 1. Schematic representation of the configuration and operational mechanism of an integrated device for capturing circulating tumor cells (CTCs). The device is composed of two functional components, a patterned silicon nanopillar (SiNP) substrate (1) with anti-EpCAM-coating exhibiting vastly enhanced CTC-capture affinity, and an overlaid microfluidic chaotic mixing chip (2) capable of promoting cell–substrate contact frequency. See text for details.

To test how the sample flow rates affect the capture efficiency of the device, cell suspensions (100 cells mL^{-1}) containing EpCAM-positive MCF7 (Figure 1) in the microchannel. Consequently, the contact frequency between CTCs and the SiNP substrate increases, resulting in enhanced CTC capture. The performance of this integrated device was first characterized with a cell suspension (100 cells mL^{-1}) of an EpCAM-positive breast cancer cell line (MCF7)[12,14,28] in cell culture medium (GIBCO DMEM medium, Invitrogen) or phosphate-buffered saline (PBS) at flow rates of 0.5–7 mL h^{-1}. An optimal flow rate (1.0 mL h^{-1}) was determined according to the resulting cell-capture efficiency. Finally, the optimal conditions were employed to capture and count CTCs from blood samples collected from prostate cancer patients with different degrees of tumor spread and with different sensitivity to treatments. The results observed by our integrated devices were compared with those observed by CellSearch assay using immunomagnetic enrichment (the only commercially available approach).[8]

The patterned SiNP substrate (Figure 1) was fabricated by combining a lithographic method and a chemical etching process (see Supporting Information). SiNPs 12 to 15 μm

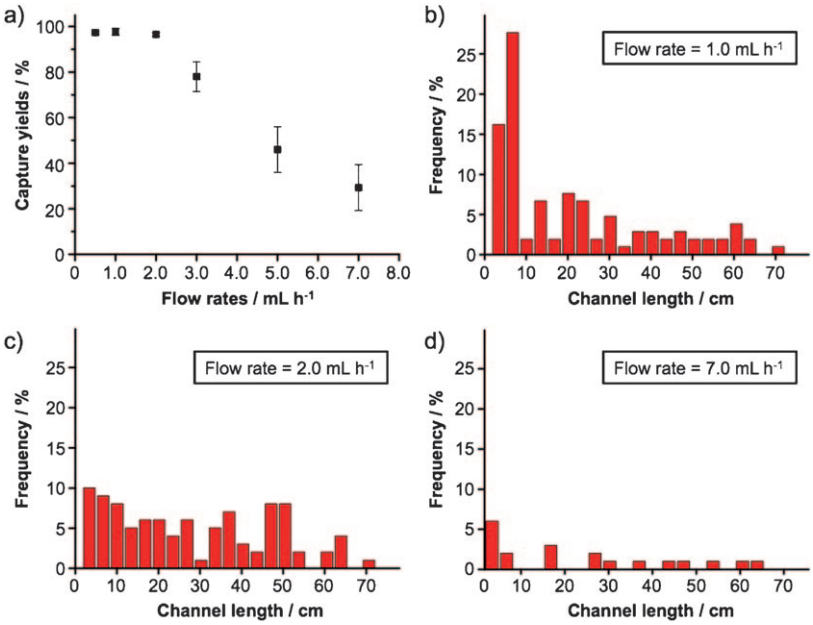

Figure 2. a) Cell-capture efficiency of the integrated CTC-capture device at flow rates of 0.5, 1, 2, 3, 5, and 7 mL h^{-1}. Error bars show standard deviations ($n = 3$). Cell suspensions (1.0 mL) containing EpCAM-positive MCF7 breast cancer cells (100 cells mL^{-1}) were employed as a model system. The error bars of the first three data points are very small. b–d) Spatial distribution of substrate-immobilized MCF7 cells along the serpentine microchannels at different flow rates of 1 (b), 2 (C), and 7 mL h^{-1} (d).

breast cancer cells in DMEM medium were introduced into the devices at flow rates of 0.5, 1, 2, 3, 5, and 7 mL h^{-1}. After rinsing, fixing, and 4',6-diamidino-2-phenylindole (DAPI) nuclear staining, the PDMS component was detached from the SiNP substrate. Subsequently, substrate-immobilized cells were imaged and counted using a fluorescence microscope. As shown in Figure 2, superb cell-capture efficiency (> 95 %) was accomplished at flow rates of 0.5, 1, and 2 mL h^{-1}. Moreover, we were able to characterize the distribution of substrate-immobilized cells at different locations of the 88 cm serpentine pattern. At a flow rate of 1 mL h^{-1} (Figure 2b), 70 % of the cells are captured in the first 25 % of the SiNP-covered microchannels. With increasing flow rates (Figure 2c,d), immobilized cells are more spread out as a result of proportionally enhanced shear forces on the immobilized cells. The cell-capture efficiency decreased at higher flow rates because of 1) reduced duration that a cell interacts with the anti-EpCAM-coated SiNP substrate (making it less likely to develop "stable" cell adhesion) and 2) increased flow-induced drag (sufficient to overcome "transient" cell adhesion). An optimal cell-capture flow rate of 1.0 mL h^{-1} was determined. To test the general applicability of these optimal cell-capture conditions, two additional EpCAM-positive cancer cell lines (PC3 prostate cancer and T24 bladder cancer cell lines) were tested in the devices with comparable cell-capture efficiency (see Figure 3a). Two control experiments based on identical design features 1) without SiNPs on the patterned substrate and 2) without the chevron-shaped micropatterns in the microfluidic channels were also conducted separately. As shown in Figure 3b, device performance was dramatically compromised, suggesting that both SiNP-based high cell-capture efficiency and micropattern-generated chaotic mixing are crucial for enhanced device performance. Finally, the cell-capture efficiency of the optimal capture conditions was validated using artificial CTC samples containing MCF7 cells. A series of MCF7-cell-spiked blood samples was prepared by spiking Red-Dye-stained MCF7 cells into blood with cell densities of approximately 50, 100, 200, and 500–1000 cells mL^{-1}. The results are summarized in Figure 3c. Regardless of whether the red blood cells were intact or lysed, optimal cell-capture conditions enabled more than 95 % recovery of cancer cells from the artificial samples. For comparison, control studies in PBS were also examined with similar cell densities.

We applied the optimized cell-capture conditions to study prostate cancer patient peripheral blood samples (Figure 4). Specifically, we attempted to validate the performance of our integrated CTC-capture platform by carrying out side-by-side comparisons with the CellSearch assay.[30] The peripheral blood samples were obtained from prostate cancer patients with different stages of the disease and under different treatments and preserved in CellSave Tubes (containing fixation agents). In each study, 1.0 mL blood was introduced into integrated devices at a back pressure ranging from 1.5 to 3.0 psi depending on the sample viscosity. After rinsing with PBS, fixation and permeabilization agents were introduced into the devices which were then incubated for 30 min. Subsequently, a commonly used three-color immunocytochemistry method was applied to identify and enumerate

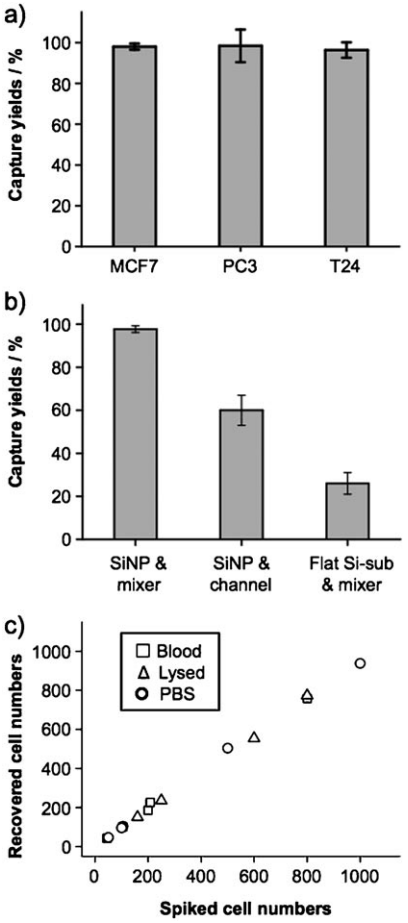

Figure 3. a) Cell-capture efficiency of the integrated CTC-capture device using suspensions of breast (MCF7), prostate (PC3), and bladder (T24) cell lines. Error bars show standard deviations ($n = 3$). b) Cell capture in the integrated CTC-capture device (SiNP & mixer) and two control devices without SiNPs on the patterned substrate (flat Si-sub & mixer) and without the chevron-shaped micropatterns in the microfluidic channels (SiNP & channel). c) Cell-capture efficiency at different cell numbers ranging from 50–1000 cells mL^{-1} in three different types of samples: whole blood (□), lysed blood (△), and PBS buffer (○).

CTCs from non-specifically trapped white blood cells (WBCs), including FITC-labeled anti-CD45 (a marker for WBCs) and PE-labeled anti-CK (Cytokeratin, a protein marker for epithelial cells) as well as DAPI nuclear staining. Fluorescence microscopy was employed to quantify[31,32] DAPI intensities and expression levels of CK and CD45 in individual cells. As shown in Figure 4a, CTCs exhibit strong CK expression and negligible CD45 signals. In contrast, WBCs present low CK and high CD45 expression levels. DAPI staining validates that the captured cells retain intact nuclei. Furthermore, the morphology and footprint sizes of the cells offer another layer of confinement for cross checking the observation from the perspectives of pathology and cytology. The combined information was utilized to delineate CTCs (DAPI + /CK + /CD45-, 40 μm > cell sizes > 10 μm) from WBCs (DAPI + /CK-/CD45 + , sizes < 15 μm) and cellular debris. The side-by-side comparison data of the inte-

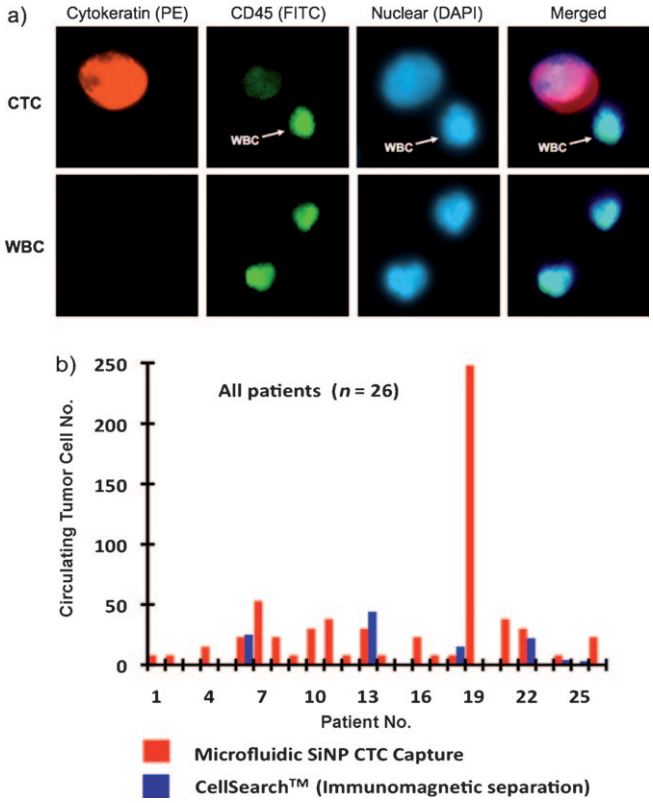

Figure 4. a) Fluorescent micrographs of CTCs captured from blood samples from a prostate cancer patient. Three-color immunocytochemistry method based on PE-labeled anti-Cytokeratin, FITC-labeled anti-CD45, and DAPI nuclear staining was applied to identify and enumerate CTCs from non-specifically trapped WBCs on the SiNP substrates. See text for details. b) Side-by-side representation of CTC enumeration results obtained from our integrated CTC-capture technology (red columns, normalized to 7.5 mL of blood) and a CellSearch assay (blue columns) on matched samples from 26 patients. The raw data without normalization from 1.0 to 7.5 mL using our integrated devices and by CellSearch assay are summarized in Supporting Information (Table S2).

grated microfluidic SiNP platform versus CellSearch is summarized in Figure 4b. Since our CTC counts were obtained from measurements using 1.0 mL blood samples, the results were normalized to CTC counts per 7.5 mL blood (the quantity routinely tested and units reported by CellSearch assay) to facilitate comparison. In 17 out of 26 patient blood samples, our platform captured significantly greater CTC numbers compared to the CellSearch assay. See Supporting Information for more details on the method comparison and clinical correlation.

In conclusion, we have demonstrated a new CTC-capture platform that combines a high-affinity cell enrichment assay based on cell capture-agent-coated nanostructured substrates and a chaotic mixing chip capable of improving CTC/substrate contact frequency. The resulting synergistic effects have led to the high CTC-capture performance observed for both spiked and clinical blood samples. We envision that the significantly improved sensitivity of our new CTC capture technology will open up opportunities for 1) early detection of cancer metastasis and 2) for isolation of rare populations of cells that cannot feasibly be done using existing technologies.

Received: September 18, 2010
Revised: November 19, 2010
Published online: March 4, 2011

Keywords: cancer diagnosis · cell capture · circulating tumor cell · microfluidics · nanostructured materials

[1] K. Pantel, R. H. Brakenhoff, *Nat. Rev. Cancer* **2004**, *4*, 448.
[2] P. S. Steeg, *Nat. Med.* **2006**, *12*, 895.
[3] C. A. Klein, *Science* **2008**, *321*, 1785.
[4] I. J. Fidler, *Nat. Rev. Cancer* **2003**, *3*, 453.
[5] R. Bernards, R. A. Weinberg, *Nature* **2002**, *418*, 823.
[6] A. C. Chiang, J. Massague, *N. Engl. J. Med.* **2008**, *359*, 2814.
[7] P. D. Bos, X. H. F. Zhang, C. Nadal, W. P. Shu, R. R. Gomis, D. X. Nguyen, A. J. Minn, M. J. van de Vijver, W. L. Gerald, J. A. Foekens, J. Massague, *Nature* **2009**, *459*, 1005.
[8] M. Cristofanilli, G. T. Budd, M. J. Ellis, A. Stopeck, J. Matera, M. C. Miller, J. M. Reuben, G. V. Doyle, W. J. Allard, L. W. M. M. Terstappen, D. F. Hayes, *N. Engl. J. Med.* **2004**, *351*, 781.
[9] K. Pantel, R. H. Brakenhoff, B. Brandt, *Nat. Rev. Cancer* **2008**, *8*, 329.
[10] D. X. Nguyen, P. D. Bos, J. Massague, *Nat. Rev. Cancer* **2009**, *9*, 274.
[11] D. Marrinucci, K. Bethel, M. Luttgen, R. H. Bruce, J. Nieva, P. Kuhn, *Arch. Pathol. Lab. Med.* **2009**, *133*, 1468.
[12] S. Nagrath, L. V. Sequist, S. Maheswaran, D. W. Bell, D. Irimia, L. Ulkus, M. R. Smith, E. L. Kwak, S. Digumarthy, A. Muzikansky, P. Ryan, U. J. Balis, R. G. Tompkins, D. A. Haber, M. Toner, *Nature* **2007**, *450*, 1235.
[13] S. Zheng, H. Lin, J. Q. Liu, M. Balic, R. Datar, R. J. Cote, Y. C. Tai, *J. Chromatogr. A* **2007**, *1162*, 154.
[14] A. Adams, P. I. Okagbare, J. Feng, M. L. Hupert, D. Patterson, J. Göttert, R. L. McCarley, D. Nikitopoulos, M. C. Murphy, S. A. Soper, *J. Am. Chem. Soc.* **2008**, *130*, 8633.
[15] P. R. Gascoyne, J. Noshari, T. J. Anderson, F. F. Becker, *Electrophoresis* **2009**, *30*, 1388.
[16] A. H. Talasaz, A. A. Powell, D. E. Huber, J. G. Berbee, K.-H. Roh, W. Yu, W. Xiao, M. M. Davis, R. F. Pease, M. N. Mindrinos, S. S. Jeffrey, R. W. Davis, *Proc. Natl. Acad. Sci. USA* **2009**, *106*, 3970.
[17] J. P. Gleghorn, E. D. Pratt, D. Denning, H. Liu, N. H. Bander, S. T. Tagawa, D. M. Nanus, P. A. Giannakakou, B. J. Kirby, *Lab Chip* **2010**, *10*, 27.
[18] S. Wang, H. Wang, J. Jiao, K. J. Chen, G. E. Owens, K. Kamei, J. Sun, D. J. Sherman, C. P. Behrenbruch, H. Wu, H. R. Tseng, *Angew. Chem.* **2009**, *121*, 9132; *Angew. Chem. Int. Ed.* **2009**, *48*, 8970.
[19] P. T. H. Went, A. Lugli, S. Meier, M. Bundi, M. Mirlacher, G. Sauter, S. Dirnhofer, *Hum. Pathol.* **2004**, *35*, 122.
[20] M. Munz, P. A. Baeuerle, O. Gires, *Cancer Res.* **2009**, *69*, 5627.
[21] K. E. Fischer, B. J. Aleman, S. L. Tao, R. H. Daniels, E. M. Li, M. D. Bunger, G. Nagaraj, P. Singh, A. Zettl, T. A. Desai, *Nano Lett.* **2009**, *9*, 716.
[22] A. D. Stroock, S. K. Dertinger, A. Ajdari, I. Mezic, H. A. Stone, G. M. Whitesides, *Science* **2002**, *295*, 647.
[23] R. H. Liu, M. A. Stremler, K. V. Sharp, M. G. Olsen, J. G. Santiago, R. J. Adrian, H. Aref, D. J. Beebe, *J. Microelectromech. Syst.* **2000**, *9*, 190.
[24] X. Z. Niu, Y. K. Lee, *J. Micromech. Microeng.* **2003**, *13*, 454.

[25] J. Liu, B. A. Williams, R. M. Gwirtz, B. J. Wold, S. Quake, *Angew. Chem.* **2006**, *118*, 3700; *Angew. Chem. Int. Ed.* **2006**, *45*, 3618.
[26] J. Wang, G. Sui, V. P. Mocharla, R. J. Lin, M. E. Phelps, H. C. Kolb, H. R. Tseng, *Angew. Chem.* **2006**, *118*, 5402; *Angew. Chem. Int. Ed.* **2006**, *45*, 5276.
[27] J. O. Foley, A. Mashadi-Hossein, E. Fu, B. A. Finlayson, P. Yager, *Lab Chip* **2008**, *8*, 557.
[28] C. G. Rao, D. Chianese, G. V. Doyle, M. C. Miller, T. Russell, R. A. Sanders, Jr., L. W. Terstappen, *Int. J. Oncol.* **2005**, *27*, 49.
[29] S. K. Murthy, A. Sin, R. G. Tompkins, M. Toner, *Langmuir* **2004**, *20*, 11649.
[30] D. R. Shaffer, M. A. Leversha, D. C. Danila, O. Lin, R. Gonzalez-Espinoza, B. Gu, A. Anand, K. Smith, P. Maslak, G. V. Doyle, L. W. Terstappen, H. Lilja, G. Heller, M. Fleisher, H. I. Scher, *Clin. Cancer Res.* **2007**, *13*, 2023.
[31] J. Sun, M. D. Masterman-Smith, N. A. Graham, J. Jiao, J. Mottahedeh, D. R. Laks, M. Ohashi, J. DeJesus, K. Kamei, K. B. Lee, H. Wang, Z. T. F. Yu, Y. T. Lu, S. A. Hou, K. Y. Li, M. Liu, N. G. Zhang, S. T. Wang, B. Angenieux, E. Panosyan, E. R. Samuels, J. Park, D. Williams, V. Konkankit, D. Nathanson, R. M. van Dam, M. E. Phelps, H. Wu, L. M. Liau, P. S. Mischel, J. A. Lazareff, H. I. Kornblum, W. H. Yong, T. G. Graeber, H. R. Tseng, *Cancer Res.* **2010**, *70*, 6128.
[32] K. I. Kamei, M. Ohashi, E. Gschweng, Q. Ho, J. Suh, J. H. Tang, Z. T. F. Yu, A. T. Clark, A. D. Pyle, M. A. Teitell, K. B. Lee, O. N. Witte, H. R. Tseng, *Lab Chip* **2010**, *10*, 1113.

